Optical and Neutron Inelastic Scattering Study of Norbornane: A New Assignment of Vibrational Frequencies

Yvon Brunel,[†] Christian Coulombeau,*[†] Christiane Coulombeau,[†] Michel Moutin,[†] and Hervé Jobic[‡,⊥]

Contribution from LEDSS VI, Domaine Universitaire, BP n° 68, 38402 Saint-Martin-D'Hères Cedex, France, L.A. 332, C.N.R.S. 15, and Institut Lauë Langevin, 156 X, 38042 Grenoble Cedex, France. *Received January 24, 1983*

Abstract: We have measured the infrared, Raman, and neutron vibrational spectra of norbornane. The lowest frequency at 172 cm^{-1} has not previously been observed. A normal coordinate analysis based on the Snyder and Schachtschneider valence force field has been carried out. The optical frequencies and neutron intensities calculated with our final force field are in good agreement with the experimental data.

Introduction

The norbornane molecule (**1**) and some of its derivatives such as the 2-methylnorbornanes (**2**, **3**) and the 2,3-dimethylnorbornanes (**4**, **5**, **6**) constitute an interesting series for studying strain energy effects. The skeletal framework of these molecules is itself a highly strained system, and the additional methyl group interactions present in the substituted compounds vary with their positions (*endo* or *exo*). The additive or specific effects of these interactions can be clarified by a comparative study of these compounds.

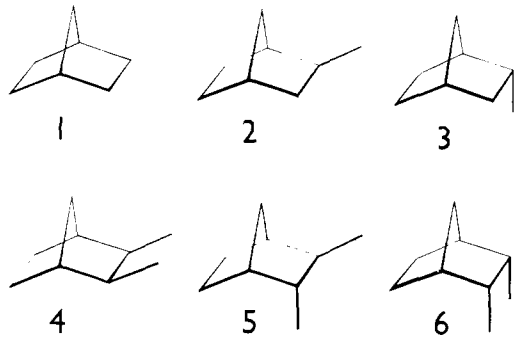

Chemical equilibration performed on the methyl norbornanes[1] and on the dimethyl norbornanes[2] is a first approach toward the correlation of the relative stabilities with molecular structure. The calculation[3] of the free enthalpy differences $\Delta G_T°$ between isomers (**2**, **3**) and (**4**, **5**, **6**) is in good agreement with the experimental values[1,2] and it satisfactorily explains the relative stabilities of these isomers.

The low-frequency vibrations give a large contribution to the enthalpy and entropy terms. They are particularly sensitive to steric interactions which are most important for isomer (**6**).[3]

In a related series of molecules, such as *endo–endo* and *exo–exo* tetracyclo[6,2,1,1,0]dodecanes, Ermer[4] reports the X-ray crystal structure and compares the results with force field calculations. He gives an interpretation of the symmetry of these molecules: the *endo–endo* compound has the C_2 symmetry, without greatly deviating from C_{2v}, while the *exo–exo* has to a good approximation, C_{2v} symmetry. Ermer gives also the calculated lowest frequency value of *endo–endo* and *exo–exo* cyclododecanes (69 and 63 cm^{-1}, respectively) which can be compared with the lowest frequency of norbornane (166 cm^{-1}) and notes that the corresponding normal coordinates involve atomic motions which minimize the hydrogen interactions in space.

In order to obtain more information on the steric interactions which occur in the norbornane derivatives, we need a complete vibrational analysis of the whole series. The first step is to determine a valence force field for norbornane which may then be transferred to the methyl derivatives.

We have measured the infrared, Raman, and neutron spectra of norbornane and we report in this paper a normal coordinate analysis based on the well-known valence force field of Snyder and Schachtschneider.[5] We have used neutron inelastic spectroscopy (NIS) because, contrary to optical methods, NIS is not bound by selection rules, and because the intensities of the vibrational transitions can be computed through the proton displacements.

Previous Results

The norbornane geometry has been established by electron diffraction[6] (see Figure 1). The strain of the ring system affects the internal coordinates and results in an increase of the CC bond lengths ($C_1C_7 = C_4C_7 = 1.57$ Å,[6a] 1.56 Å [6b]) and in a decrease of the CCC bridge angle ($C_1C_7C_4 = 94°$,[6a] 96°[6b]) Molecular mechanics calculations[7] do not account for the differences between these values and the more usual ones. However, Ermer's calculations[8] have shown a relationship between cross terms such as bond angle force constants and CC bond lengths obtained after minimization of energy.

Two different force fields have been proposed for this molecule; Levin and Harris have published the IR and Raman spectra of norbornane along with a normal coordinate analysis[9] and almost at the same time Meic et al. reported preliminary work using the Snyder and Schachtschneider force constants.[10] However, it appears that the low-frequency vibrations, which have a low intensity in the optical spectra, may not be correctly assigned. For example, the lowest A_2 frequency, which is calculated at 348 cm^{-1} by Levin and Harris,[9] is found at 93 cm^{-1} by Meic et al.[10] (com-

[†] LEDSS VI.
[‡] Institut Lauë Langevin.
[⊥] Present adress: Institut de Recherche sur la Catalyse, 2 Av. Albert Einstein, 69626 Villeurbanne Cedex.

(1) R. J. Ouelette, J. D. Rawn, and S. N. Jreissaty, *J. Am. Chem. Soc.*, **93**, 7117 (1971).
(2) N. A. Belikova, L. I. Kovalenko, M. A. Moskaleva, M. Ordubadu, A. F. Plate, Kh. E. Sterin, and R. S. Yagminas, *Zh. Org. Khim.* **4**, 1363 (1968).
(3) Y. Brunel, C. Coulombeau, and A. Rassat, *Nouv. J. Chim.*, **4**, 663 (1980).
(4) O. Ermer, *Angew, Chem. Int. Ed. Engl.*, **16**, 798 (1977).
(5) R. G. Snyder and J. H. Schachtschneider, *Spectrochim. Acta*, **21**, 169 (1965).
(6) (a) A. Yokozeki and K. Kuchitsu, *Bull. Chem. Soc. Jpn.*, **44**, 2356 (1971); (b) J. F. Chiang, C. F. Wilcox, Jr., and S. H. Bauer, *J. Am. Chem. Soc.*, **90**, 3149 (1968).
(7) (a) N. L. Allinger, M. T. Tribble, M. A. Miller, and D. H. Wertz, *J. Am. Chem. Soc.*, **92**, 1637 (1970); (b) N. L. Allinger and J. T. Sprague, *J. Am. Chem. Soc.*, **94**, 5734 (1972); (c) E. M. Engler, J. D. Andose, and P. Von R. Schleyer, *J. Am. Chem. Soc.*, **95**, 8005 (1973).
(8) O. Ermer, *Tetrahedron*, **30**, 3103 (1974).
(9) I. W. Levin and W. C. Harris, *Spectrochim, Acta*, **29A**, 1815 (1973).
(10) Z. Meič, M. Randič, and A. Rubcič, *Croat. Chem. Acta*, **46**, 25 (1974).

0002-7863/83/1505-6411$01.50/0

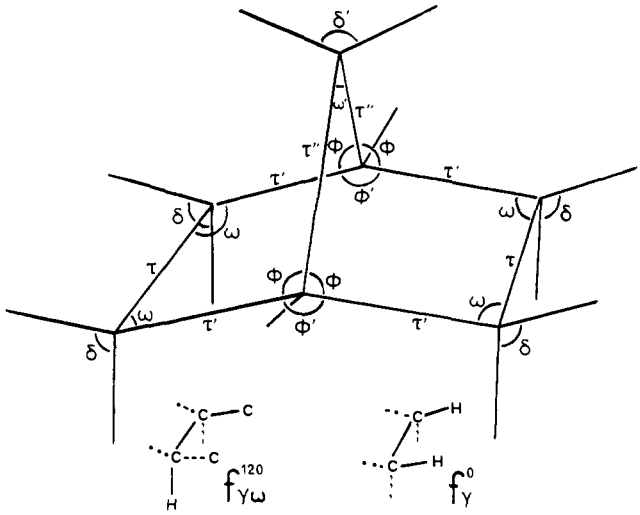

Figure 1. Internal coordinates defined several times in norbornane. CCC angles of 2-bridge and 1-bridge ω and ω'; CCC angles of bridgehead ϕ and ϕ'. HCH angles of methylenes of 2-bridge and 1-bridge δ and δ', respectively; dihedral torsions τ, τ', τ''. Two cross terms $f_{\gamma\omega}^{120}$ and f_{γ}^{0} centered on adjacent carbons are also defined.

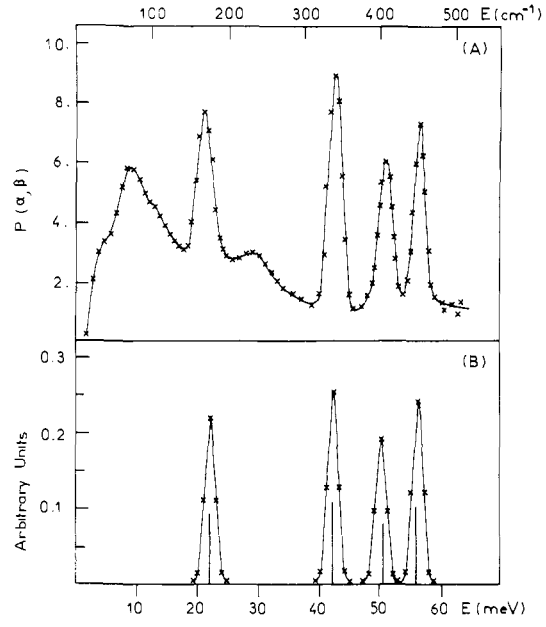

Figure 2. (a) NIS spectrum of norbornane obtained on IN4 at 6 K. (b) Calculated spectrum.

pared with a value of 166 cm^{-1} obtained by Ermer[4]). This optically inactive vibration and the other low-frequency modes should be observed in the NIS spectrum because they involve large hydrogen displacements.

Experimental Section

For internal consistency, we have again measured the infrared and Raman spectra. The NIS spectra were obtained at the Institut Lauë Langevin, Grenoble.

1. Optical Spectra. The infrared spectra were obtained on two different spectrometers. The vibrational range 240–4000 cm^{-1} was investigated with a Perkin-Elmer 180 spectrometer; the sample, at room temperature, was maintained between CsI windows. The low frequencies were recorded from 20 to 360 cm^{-1} with a Polytec FIR 30; the norbornane pellet (obtained with a pressure of 250 kg cm^{-2}) was placed between polyethylene windows.

The Raman spectra were obtained with a Coderg PHO spectrometer powered by a Spectra Physics argon ion laser operating at 5145 Å. The spectra were recorded with the pure sample in the liquid (360 K) and solid (100 K) phases. The depolarization ratios were checked with a solution in CCl_4 or C_6H_6. All samples were contained in sealed glass tubes.

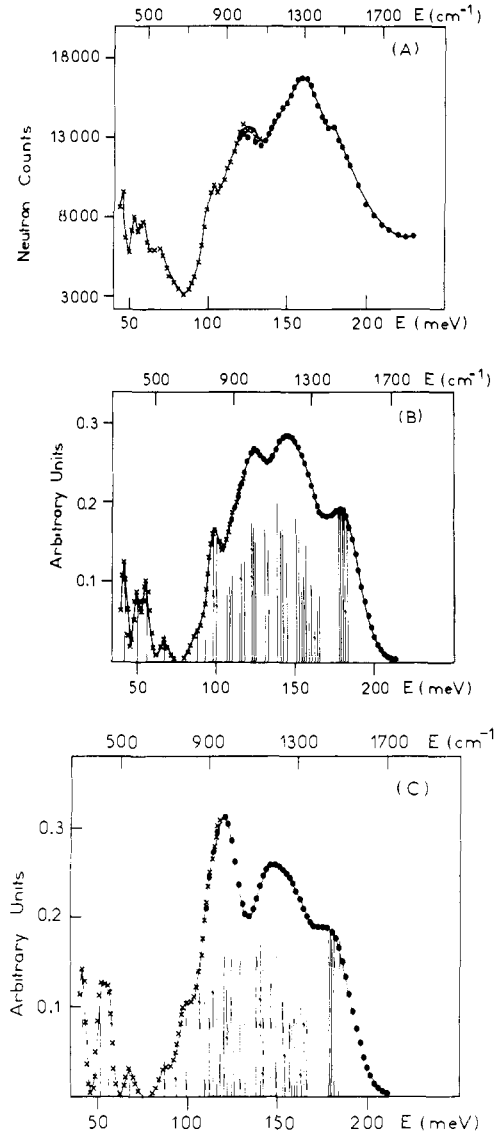

Figure 3. (a) NIS spectrum of norbornane obtained on IN1 at 80 K, (×) and (●) points obtained with the (200) and (220) copper planes, respectively. (b) Spectrum calculated from the final assignment. (c) Spectrum calculated from the intermediate assignment (see text).

2. NIS Spectra. The NIS spectra were obtained on two different spectrometers at the I.L.L.; the low-frequency region was investigated on IN4 at 6 K, and the high-frequency range on IN1 at 80 K. The powder sample, which was contained in an aluminum cell, was made up to scatter about 15% of the incident beam.

IN4 is a down-scattering time-of-flight spectrometer installed on a thermal neutron beam-tube.[11] The incident energy, which is defined by two copper monochromators, was taken as 550 cm^{-1} to obtain a region of overlap with the data from IN1. The analysis of time-of-flight data was performed using I.L.L. standard programs.[12] The spectrum which is presented in Figure 2(a) is a summation of the data from the detectors placed between 10 and 70°. The instrumental resolution $\Delta E/E_0$ is of the order of 4% in the inelastic region. The frequencies of the vibrations are thus given with a precision of about 10 cm^{-1}.

IN1 is a beryllium filter detector spectrometer mounted on a beam-tube facing the hot source.[11] The incident neutron energy is selected by Bragg scattering from the (200) and (220) planes of a copper monochromator giving energies ranging from 300 to 2000 cm^{-1}. After scattering by the sample, the neutrons must pass through a cooled beryllium block before detection. Only neutrons which have lost energy due to a vibrational transition, giving a final energy of about 30 cm^{-1} are transmitted for detection. The spectrum presented in Figure 3(a) is thus

(11) Neutron beam facilities at the HFR available for users, I.L.L., (Internal Scientific Report 1981).

(12) H. Jobic, J. Tomkinson, and A. Renouprez, *Mol. Phys.*, **39**, 989 (1980).

Table I. Infrared, Raman, and Neutron Frequencies for Norbornane Along with the Relative Intensities and Polarization Ratios (I_P/I) for the Raman Bands in Solution. The Final Assignment Is Indicated

infrared, solid, FIR	infrared in soln, NIS*	I	Raman, solid	I	Raman, liquid	Raman, in soln	I	I_P	I_P/I	assignment
			2967	100	2971		100.0			
					2963		100.0	20.0	0.20	$\nu_1\nu_{16}\nu_{27}\nu_{40}$
	2960	vs	2957	72						
			2950	40						ν_{41}
	2940	vs	2941	36						
			2933	50	2935		70.0	12.0	0.17	
					2919		25.0	1.0	0.04	ν_2
	2913	vs	2914	16						
					2901		25.0	1.0	0.04	$2 \times 1450 = 2900$
			2897	14						ν_{28}
	2865	vs	2870	52	2873		75.0	4.0	0.05	$\nu_3\nu_4\nu_{17}\nu_{29}\nu_{42}$
						1483	3.0	1.2	0.4	ν_5
	1462	s	1460	8						
	1455	s	1453	24						
	1449	s			1450	1450	10.0	7.6	0.76	$\nu_6\nu_{18}\nu_{30}$
	1447	s								
			1443	20						ν_{43}
			1428	1						$891 + 542 = 1433$
1400		w			1400					$950 + 454 = 1404$
			1323	6						$\nu_{19}\nu_{44}$
1310	1310	m	1319	8	1317	1320	4.5	3.0	0.67	ν_7
			1283	1						ν_{31}
			1278	1						ν_{32}
			1270	1		1272	1.5	0.9	0.6	ν_{20}
1253	1252	w	1260	1		1255	2.5	0.9	0.36	ν_8
1238	1236	w	1244	18	1237	1240	3.9	3.0	0.77	ν_{45}
			1220	17		1214	4.8	3.6	0.75	ν_{21}
1203	1207	m	1209	1	1211					ν_{33}
1165		w	1163	2		1162	1.8	1.5	0.83	ν_{34}
	1157	m								
1145		m	1147	18	1141	1145	7.6	5.8	0.77	$\nu_9\nu_{46}$
	1139	m								
			1130	2						$451 + 2 \times 342 = 1135$
			1123	22						ν_{22}
					1119	1118	10.0	7.6	0.76	
1110		w	1116	<1						$172 + 950 = 1122$
1070	1070	m	1073	11		1074	4.8	3.6	0.75	$\nu_{35}\nu_{47}$
					1064					
1022	1022	s	1033	18	1025	1024	6.5	4.8	0.74	ν_{36}
	1005	vw								
988			995	58	992	993	26.0	17.4	0.67	$\nu_{10}\nu_{23}$
			961	6	967	967	0.2			ν_{24}
948	950	s	950	12	952	954	12.0	7.2	0.60	ν_{48}
920	921	s	924	51	922	923	100.0	1.8	0.02	ν_{11}
			918							$754 + 172 = 926$
888	888	m	891	6		890	2.4	1.8	0.75	ν_{37}
870	872	m	875	52	871	874	20.0	2.4	0.12	$\nu_{12}\nu_{49}$
814	817	m	814	2	817	815	16.0	1.8	0.11	ν_{13}
798		w								$454 + 342 = 796$
786	787	m	791	1	786					ν_{50}
754	755	s	754	16	755	754	42.0	15.0	0.36	ν_{14}
700		vw	700	<1	696	703				ν_{38}
			625	<1						$454 + 172 = 626$
			585	<1						$410 + 172 = 582$
	540		541	1		541	5	0.3	0.6	ν_{25}
			520	<1						$342 + 172 = 514$
	450*		454	3	445	448	1.3	1.0	0.77	ν_{51}
406	410*	vw	411	5	409	408	4.2	1.2	0.29	ν_{15}
340,333	342*	w	342	51		343	1.0	0.7	0.75	ν_{39}
	172*					164	0.7	0.57	0.81	ν_{26}

shifted up by this value, but the frequencies quoted here are corrected for this. The resolution function that we use to calculate the vibrational spectrum includes the instrumental resolution and the intrinsic width of the modes;[13] it is of about 8% of the incident energy E_0.

The neutron spectra are recorded at lower temperatures than the optical data to sharpen the peaks and to reduce the influence of the Debye–Waller factor.[14] This may induce small shifts of a few wavenumbers for the internal modes, as shown in Table I for the Raman frequencies in the liquid and solid phases. However, these small differences cannot modify our assignment and because they are of the same magnitude as the frequencies accuracy, they are not important for our refinement. The observed optical and neutron frequencies are listed in Table I.

Calculation of the One-Phonon Neutron Spectrum

Because of the relatively large incoherent cross section (σ_H) and the low mass of the hydrogen atom (m_H), only the incoherent scattering from hydrogen has to be considered. The scattering due to the carbon atoms can be neglected. In the isotropic approximation, the partial differential cross section $d^2\sigma/d\Omega dE$, which

(13) A. Griffin and H. Jobic, *J. Chem. Phys.*, **75**, 5940 (1982).
(14) H. Jobic, R. E. Ghosh, and A. Renouprez, *J. Chem. Phys.*, **75**, 4025 (1981).

Table II. Valence Force Constants for Norbornane. The Notation and the Initial Values Are Taken from Ref 5. The Force Constants Are in mdyn Å^{-1}, the Deformations in mdyn Å rad^{-2} and the Bond-Angle Interactions in mdyn rad^{-1}

force const	init value (ref 5)	final value	force const	init value (ref 5)	final value
K_d	4.554	4.6318	F_R	0.101	0.0346
K_s	4.588	4.5759	F_d	0.006	−0.0345
K_R	4.387	4.2325	$F_{R\gamma}$	0.328	0.2578
K_R'	4.337	4.5207	$F_{R\omega}$	0.417	0.4370
H_δ	0.550	0.5824	$F_{R\gamma'}$	0.079	0.0973
H_γ	0.656	0.6095	F_γ	−0.021	−0.0709
H_ζ	0.657	0.5590	F_ϕ	−0.041	0.2812
H_ω	1.130	0.6780	$F_{\gamma'}$	0.012	−0.0084
H_ω'	1.130	0.6175	$F_{\gamma\omega}$	−0.031	−0.0702
H_ϕ	1.084	1.8739	f_γ^g	−0.005	0.0092
H_ϕ'	1.084	1.4604	f_γ^0		−0.0468
H_τ	0.072	0.0551	$f_{\gamma\omega}^{120}$		0.1058
H_τ'	0.072	0.1020	$f_{\gamma\omega}^t$	0.049	−0.0199
H_τ''	0.072	0.0617	$f_{\gamma\omega}^g$	−0.052	−0.0473

represents the fraction of neutrons scattered into the solid angle $\Delta\Omega$ and with energy in the range ΔE, may be written[15]

$$\frac{d^2\sigma}{d\Omega dE} = \frac{k}{2k_0}\frac{\sigma_H}{4\pi}\sum_{d,\lambda}\exp(-2W_d)\frac{K^2C_d^2(\lambda)}{2m_H\omega_\lambda}\delta(\omega-\omega_\lambda)$$

It should be noted that this expression is obtained in the harmonic approximation and for one phonon down-scattering processes. The neutron momentum transfer $\hbar\boldsymbol{K}$ is defined by $\boldsymbol{K} = \boldsymbol{k}_0 - \boldsymbol{k}$, where $\boldsymbol{k}_0$ and $\boldsymbol{k}$ are respectively the incident and final wave vectors. One of us has recently shown that the influence of the Debye–Waller factor, $\exp(-2W_d)$, for atom d may be neglected when comparing experimental and calculated spectra.[13,14] The intensities of the δ functions, corresponding to the internal vibrations ω_λ, are thus governed by the mass-weighted eigenvectors $C_d(\lambda)$. These vectors which describe the atomic displacements can be computed from an existing force field, using the well-known **G F** matrix method.[16]

Force Field Description

The initial force constants are taken from the work of Snyder and Schachtschneider on saturated hydrocarbons.[5] Their original notation is used (see Table II).

We have considered all the different internal coordinates, including eight torsions. We have retained all the redundancies in order to assure the maximum of transferability of the valence force constants.

Our intention is to use our final force field to analyze the spectra of the methyl norbornanes. Because these derivatives have a lower symmetry than norbornane, we did not construct the symmetry coordinates. The structural parameters were taken from the electron diffraction data of Chiang et al.[6b] The internal coordinates which are defined several times on the basis of the norbornane symmetry are presented in Figure 1. We have differentiated: (i) four constants corresponding to the CCC angles: H_ω, $H_{\omega'}$, H_ϕ and $H_{\phi'}$; (ii) three torsional force constants: H_τ, $H_{\tau'}$, and $H_{\tau''}$. Due to the geometry of norbornane, we have also defined two interaction force constants $f_\gamma{}^0$ and $f_{\gamma\omega}{}^{120}$, which are also depicted in Figure 1.

Compared with the force field of Snyder and Schachtschneider,[5] we have neglected a few interaction constants whose influence was small. During the perturbation, additional force constants were investigated, but we found that these terms did not improve the fit very much. In the final calculation, we end up with 28 force constants; the resulting force field is shown in Table II.

(15) M. W. Thomas and R. E. Ghosh, *Mol. Phys.*, **29**, 1489 (1975).
(16) E. B. Wilson, J. C. Decius, and P. C. Cross, "Molecular Vibrations", McGraw-Hill, New York 1955.

Results

1. Vibrational Assignment. The norbornane molecule belongs to the C_{2v} point group. The 51 fundamental vibrations are distributed over the symmetry types as

$$\Gamma_v = 15A_1 + 11A_2 + 13B_1 + 12B_2$$

All the vibrations are Raman active but the A_2 modes are infrared inactive. An unambiguous assignment of all the vibrational modes of such a complex molecule is obviously difficult to obtain. However, compared to the work of Levin and Harris,[9] we have supplementary data, i.e., the peak positions and intensities of the neutron bands.

Thus, in the neutron spectrum which is presented in Figure 2(a), we find a well-defined peak at 172 cm^{-1} (a vibration that has not been observed previously). This peak can be readily assigned to the lowest A_2 mode. This mode cannot be found in the FIR spectrum. It has a weak Raman intensity but nevertheless it can be observed for norbornane in solution. The frequency of this A_2 mode is in excellent agreement with the value of 166 cm^{-1} calculated by Ermer.[4] The weak band which is observed at about 230 cm^{-1} in the NIS spectrum, Figure 2(a), results from the combination of the mode at 172 cm^{-1} with the lattice modes, the frequency distribution of which peaks at about 70 cm^{-1}. On the other hand, we could not find, by any spectroscopy, the weak Raman band observed by Levin and Harris at 487 cm^{-1}.[9] Therefore this frequency was not included in our refinement.

Our starting assignment was based first on the lowest frequency modes observed by NIS, because the resolution is reasonably good below 700 cm^{-1}. The depolarization ratio of the Raman band measured at 410 cm^{-1} confirms that it is an A_1 mode. Further, the vibration observed at 542 cm^{-1} in the Raman and NIS spectra, but not in the infrared spectrum, implies that it is an A_2 mode. We also took into account the other A_1 modes which were associated with the polarized Raman bands, and the A_2 modes which were determined after a comparison of the infrared and Raman frequencies.

The assignment of the B_1 and B_2 modes was changed at various stages of the refinement, and even the assignment of a few A_1 modes had to be modified.

The assignment was progressively clarified by a coupled calculation of the optical frequencies and of the neutron scattering intensities. The neutron spectrum above 700 cm^{-1} contains only a few broad bands as shown in Figure 3(a). This is partly due to the relatively poor resolution in that range but also to the large number of vibrational modes. However, this spectrum proved to be very useful because the profile of the calculated neutron spectrum is rather sensitive to the vibrational assignment.

We now give an example of the comparison between the experimental neutron spectrum and two calculated neutron spectra derived from two different assignments.

In our first assignment, we have considered that the polarized Raman band at 816 cm^{-1} was the first overtone of the A_1 mode at 410 cm^{-1}. This was the assignment taken by Levin and Harris.[9] The other A_1 modes were placed at 754, 875, 923, 950, and 992 cm^{-1}. From this assignment, an average error of 0.61% was obtained. The resulting calculated neutron spectrum is shown in Figure 3(c). The spikes correspond to the different vibrational modes and the convolution with the experimental resolution function yields the continuous profile. It can be seen that the agreement with the experimental spectrum, Figure 3(a), is not satisfactory: the shoulder at 800 cm^{-1} is too weak and the peak at 960 cm^{-1} is too large.

We then considered a second assignment where the polarized Raman band at 816 cm^{-1} is taken as a fundamental (the other A_1 modes are then situated at 754, 875, 923, and 992 cm^{-1}...). The complete assignment is given in Table III. The neutron spectrum calculated from the refined force field is presented in Figure 3(b). We now obtain a better agreement with the experimental spectrum: the peak at 800 cm^{-1} is more intense and the intensity of the peak at 960 cm^{-1} has decreased. Further, the low-frequency spectrum calculated with the same force field,

Table III. Observed and Calculated Vibrational Modes for Norbornane (in cm^{-1}) along with Their Potential Energy Distribution (P.E.D.) and an Approximate Description: ν = stretching, s = scissoring, w = wagging, t = twisting, r = rocking modes; δ and δ' Refer to Methylene HCH Angles; bh = bridgehead, def = Deformation, sk = Skeletal

no. of vibr		obsd	calcd	potential energy distribution	approx description	$\Sigma C_d^2(\lambda)$ H
A_1	ν_1	2965	2960	K_d (99)	ν_{CH}	0.99
	ν_2	2914	2907	K_s (98)	ν_{CH}	0.98
	ν_3	2870	2873	K_d (100)	ν_{CH}	0.99
	ν_4	2870	2870	K_d (100)	ν_{CH}	0.99
	ν_5	1483	1482	H_δ (77), H_γ (27)	$s_{\delta'}$	0.93
	ν_6	1451	1446	H_δ (81), H_γ (24)	s_δ	0.93
	ν_7	1319	1314	K_R (32), $K_{R'}$ (28), H_γ (39)	ν_{CC}	0.18
	ν_8	1256	1253	$K_{R'}$ (28), H_γ (45), H_ξ (28)	bh def + t_δ	0.72
	ν_9	1145	1135	$K_{R'}$ (15), H_γ (45), H_ξ (38)	t_δ + bh def	0.81
	ν_{10}	992	997	$K_{R'}$ (10), H_γ (61), H_ξ (18)	w_δ	0.87
	ν_{11}	923	929	$K_{R'}$ (61), H_γ (10), H_ξ (11)	ν_{CC}	0.32
	ν_{12}	875	879	K_R (37), $K_{R'}$ (28), H_γ (27)	ν_{CC}	0.46
	ν_{13}	816	809	$K_{R'}$ (13), H_γ (62)	r_δ	0.63
	ν_{14}	754	752	K_R (12), $K_{R'}$ (28), H_ϕ (24), $H_{\omega'}$ (10)	sk def	0.14
	ν_{15}	410	409	H_γ (11), H_ϕ (23), $H_{\phi'}$ (81)	"butterfly"	0.41
A_2	ν_{16}	2965	2965	K_d (98)	ν_{CH}	0.98
	ν_{17}	2870	2869	K_d (100)	ν_{CH}	0.99
	ν_{18}	1461	1457	H_δ (70), H_γ (24)	s_δ	0.90
	ν_{19}	1323	1330	$K_{R'}$ (47), H_δ (12), H_γ (37), H_ξ (22)	ν_{CC}	0.42
	ν_{20}	1270	1253	H_γ (68), H_ξ (32)	bh def	0.52
	ν_{21}	1220	1218	H_γ (79)	t_δ	0.90
	ν_{22}	1123	1124	H_γ (61), H_ξ (28)	$t_{\delta'}$	0.99
	ν_{23}	990	1005	H_γ (67), H_ξ (10)	$w_\delta + r_\delta$	0.73
	ν_{24}	960	932	$K_{R'}$ (46), H_γ (45)	$w_\delta + r_\delta$	0.61
	ν_{25}	542	547	H_γ (12), H_ω (39), H_ϕ (50)	sk def	0.16
	ν_{26}	172	178	H_ϕ (16), H_τ (21), $H_{\tau''}$ (47)	τ	0.47
B_1	ν_{27}	2965	2968	K_d (98)	ν_{CH}	0.99
	ν_{28}	2897	2905	K_s (98)	ν_{CH}	0.99
	ν_{29}	2870	2870	K_d (100)	ν_{CH}	0.98
	ν_{30}	1451	1452	H_δ (76), H_γ (23)	s_δ	0.93
	ν_{31}	1283	1288	$K_{R'}$ (38), H_γ (65)	w_δ	0.47
	ν_{32}	1278	1280	$K_{R'}$ (55), H_γ (48), H_ϕ (17)	ν_{CC}	0.24
	ν_{33}	1208	1225	H_γ (78)	t_δ	0.77
	ν_{34}	1163	1170	$K_{R'}$ (10), H_γ (47), H_ξ (35)	r_δ	0.62
	ν_{35}	1074	1075	H_γ (34), H_ξ (43)	bh def	0.70
	ν_{36}	1023	1003	H_γ (67), H_ξ (12)	$w_{\delta'}$	0.83
	ν_{37}	891	887	$K_{R'}$ (51), H_γ (34)	ν_{CC}	0.53
	ν_{38}	700	701	$K_{R'}$ (36), H_γ (15), H_ω (30)	sk def	0.23
	ν_{39}	342	339	H_ϕ (24), $H_{\phi'}$ (55), H_τ (16)	τ	0.54
B_2	ν_{40}	2965	2965	K_d (98)	ν_{CH}	0.99
	ν_{41}	2950	2957	K_d (99)	ν_{CH}	0.99
	ν_{42}	2870	2971	K_d (100)	ν_{CH}	0.98
	ν_{43}	1443	1444	H_δ (82), H_γ (24)	s_δ	0.93
	ν_{44}	1323	1325	$K_{R'}$ (48), H_γ (26), H_ξ (29), H_ϕ (12)	ν_{CC}	0.31
	ν_{45}	1244	1251	K_R (39), H_γ (38), H_ξ (34)	bh def	0.44
	ν_{46}	1147	1144	H_γ (77), H_ξ (13)	t_δ	0.94
	ν_{47}	1074	1058	H_γ (73), H_ξ (18)	w_δ	0.83
	ν_{48}	950	955	$K_{R'}$ (27), H_γ (58)	$r_{\delta'}$	0.62
	ν_{49}	872	867	K_R (55), $K_{R'}$ (22), H_γ (16)	ν_{CC}	0.41
	ν_{50}	788	792	H_γ (87)	r_δ	0.84
	ν_{51}	451	448	H_γ (12), H_ϕ (92)	bh def	0.52

Figure 2(b), agrees well with the experimental spectrum obtained on IN4, Figure 2(a).

We are aware that the assignment of some of the high-frequency modes (the CH stretching region will be discussed in the next paragraph) may not be definitive. Unfortunately, the resolution of the NIS spectrum is not sufficient above 1000 cm^{-1} and the multiphonon effects have a large contribution in that range (i.e., at high momentum transfers). The few ambiguities that remain can only be removed by using new experimental data, for instance isotopic substitution.

2. Description of the Vibrational Modes. The CH stretching vibrations were difficult to assign because of the presence of overtones and Fermi resonance. Several intense lines can be observed in the Raman spectrum, but all these bands are highly polarized. Because we expect only four A_1 modes, this indicates (i) that combination peaks are present and (ii) that the intensities of the A_2, B_1, and B_2 modes are weak. The NIS spectrum is unhelpful because only one broad band containing all the modes is obtained in this frequency range.[14] A simplified assignment was thus made in that region.

The CH_2 scissoring modes occur in the range 1440–1483 cm^{-1}; they are pure modes. Accidental degeneracy is observed for the 2-bridge methylene groups; however, the vibration corresponding to the 1-bridge CH_2 group is shifted to 1483 cm^{-1}. Such a value was found by the first normal coordinate analysis using the original force constants and we have also set $H_\delta = H_{\delta'}$ in the final calculation. The other deformation modes are a mixture of CH_2 wagging (w), twisting (t), rocking (r) and CH bending. However, we indicate in Table III which of coordinates are most involved in the different modes.

The skeletal stretches are also mixed, but the A_1 modes can be easily associated with the intense and polarized Raman bands. As already noticed by Levin and Harris,[9] only the modes at 923 and 875 cm^{-1} have a correct potential energy distribution (P.E.D.).

The skeletal deformations, which are expected at low frequencies, are all observed. They correspond to skeletal stretches

and bendings (754, 700, 542 cm^{-1}) to bridgehead deformation (451 cm^{-1}), to the "butterfly" motion (410 cm^{-1}) and to the torsions (342 and 172 cm^{-1}).

Discussion

The final force field is given in Table II. The calculated frequencies are compared with the experimental values in Table III. The average error is 0.57% or 5.55 cm^{-1}. The main contributions to the potential energy distribution are also listed in Table III together with an approximate description of the modes and with the calculated neutron intensity which is related to $\sum_H C_d^2(\lambda)$.

The valence force field of Snyder and Schachtschneider was thus a very reasonable model for norbornane, but several adjustments were necessary in order to describe the vibrations of this strained molecule.

If we compare our final constants with the original values, we find that several constants have the same order of magnitude: the stretching force constants as well as the bending constants H_γ, H_ζ and H_δ. The two constants H_δ and $H_{\delta'}$, corresponding to the two types of methylene groups (2-bridge and 1-bridge) were initially allowed to float. Since the final values were almost identical, we considered only one constant for the HCH deformations.

We find that other constants are more variable, e.g., the CCC bending force constants H_ω and H_ϕ. The values corresponding to 1-bridge and 2-bridge carbon atoms decrease, whereas they increase for the bridgehead carbon atoms (the latter atoms positions are the most deformed from a tetrahedral geometry). These CCC constants are related to the twisting force constants (H_τ, $H_{\tau'}$, $H_{\tau''}$) which have a mean value of the same magnitude as for the original model.

The interaction constants do not vary significantly except F_ϕ which has a larger value due to the major role of the bridgehead deformations. The magnitude of all the interaction force constants is reasonable and this is reflected by the values of the sums of the diagonal potential energies which are close to 100%.

Conclusion

We have shown that the low-frequency vibrations of norbornane can be assigned with certainty with the help of the NIS spectra. For the range 700–1500 cm^{-1} the NIS spectrum was also of great value as a complement to the infrared and Raman data. We have modified the valence force field of Snyder and Schachtschneider to take into account the strain of the molecule.

The force field presented in this study is of course not unique[17] because of possible assignments problems and because we have used a General Valence Force Field. However, it accounts well for the observed optical frequencies and the neutrons intensities. This new force field will be used to interpret the IR, Raman, and NIS spectra of the mono and dimethyl derivatives.

Acknowledgment. We are very much indebted to A. Chosson and A. Corne (Laboratoire de Spectroscopie Optique, Université de Savoie, Chambéry, France) for their help in recording the Raman spectra. We thank Dr. J. C. Lassègues and Dr. B. Desbat (Laboratoire de Spectroscopie Infrarouge, Bordeaux, France) for their careful reinvestigation of the infrared spectra, and Dr. Ermer for details on his calculations. Finally, we thank Professor A. Rassat for his continuous interest in this work.

Registry No. Norbornane, 279-23-2; neutron, 12586-31-1.

(17) Since this paper was originally submitted, a new molecular structure of norbornane has been published by L. Doms, L. Van den Enden, H. J. Geise, and C. Van Alsenoy, *J. Am. Chem. Soc.*, **105**, 158 (1983). This new geometry, which is derived from an extensive study of experimental and theoretical results, would slightly modify our force field. However, their set of vibrational amplitudes, from which the vibrational amplitudes are computed, is not entirely correct as we show in this paper.

Effect of Crystal Packing on the Solid-State Spectral Properties of Vicinal Diketones[1]

John I. Crowley,* Richard D. Balanson, and James J. Mayerle

Contribution from the IBM Research Laboratory, San Jose, California 95193.
Received March 21, 1983

Abstract: X-ray crystal structures are reported for six substituted benzils: 4,4'-dimethoxy (**1**), 4-ethoxy (**7**), 4,4'-diethoxy (**6**), and the meso (**4b**), racemic (**4a**), and LL chiral (**4c**) bis-4,4'-(2,2'-dimethyl-1,3-dioxacyclopentyl-4-methoxy) benzils. The syntheses of **4a**, **4b**, and **4c** are described as well as the separation of **4a** and **4b**. Crystal structure data follow. **1**: a = 21.934 Å, b = 4.064 Å, c = 15.208 Å, β = 102.11°, $C2/c$, Z = 4. **6**: a = 14.512 Å, b = 4.795 Å, c = 22.089 Å, β = 98.82°, $C2/c$, Z = 4. **7**: a = 7.577 Å, b = 14.845 Å, c = 12.153 Å, β = 97.63°, $P2/n$, Z = 4. **4a**: 10.044 Å, b = 5.339 Å, c = 22.83 Å, β = 95.84°, $P2/n$, Z = 2. **4b**: a = 22.826 Å, b = 11.067 Å, c = 9.506 Å, β = 97.03°, $P2_1/c$, Z = 2. **4c**: a = 5.390 Å, b = 10.487 Å, c = 43.985 Å, $P2_12_12_1$, Z = 4. The packing modes tend to be dominated by van der Waals close packing considerations and the preference for aligning substituted phenyl rings parallel to each other at about 3.45–3.70 Å separation. Our results afford semiquantitative support for the proposition that the solid-state color of dicarbonyl compounds is red-shifted by increased overlap and blue-shifted by decreased overlap of the carbonyls. In the case of sheets of stacked substituted benzils, the increased size of the remote substituent is accommodated in the stack by increased twisting of the carbonyls while maintaining close packing of the phenyl rings.

Introduction

The solid state colors of 4,4'-substituted benzils range from the yellow of anisil and dinitrobenzil to essentially colorless compounds. An early, erroneous explanation[2] attributed yellow colors to the presence of unsubstituted dicarbonyls while the less colored or colorless compounds were explained by substituents on the dicarbonyl chromophore which were electron donating and which "neutralized" the effect of the carbonyls. Subsequently, Leonard and associates[3] explained the variation of color as resulting from

(1) Preliminary reports of this work have been presented, in part, at the 174th National Meeting of the American Chemical Society, Chicago, IL, Aug 28–Sept 2, 1977; paper 161, Division of Physical Chemistry; 178th National Meeting of the American Chemical Society, Washington DC Sept 9–14, 1979; paper 212.

(2) Robinson, R. "Outline of an Electrochemical Theory of the Course of Organic Reactions"; Institute of Chemistry of Great Britain and Ireland: London, 1932; p 30.

0002-7863/83/1505-6416$01.50/0